

## Analyse of LHCD efficiency on the FT-2 tokamak

S.I Lashkul, A.B. Altukhov, A.D. Gurchenko, V.V. Dyachenko,  
 L.A. Esipov, M.Yu. Kantor, D.V. Kouprienko, M.A. Irzak, A.N Saveliev,  
 A.V. Sidorov, S.V. Shatalin<sup>\*</sup>, A.Yu. Stepanov

*A.F.Ioffe Physico-Technical Institute, 194021, St.Petersburg, Russia*

*\*St.Petersburg State Polytekhnical University, St.Petersburg, Russia*

At the FT-2 tokamak, where sufficiently large experience in the observations of LH wave - plasma interaction has been accumulated, long experimental series of LHCD efficiency study are carried out [1, 2]. The FT-2 tokamak with the circular cross-section and limiter configuration operates under the basic parameters:  $I_{pl} = 19 \div 40$  kA,  $B_T = 2 \div 3$  T,  $R = 0.55$  m,  $a_L = 0.08$  m,  $q = 4 \div 6$  and plasma current pulse duration  $\Delta t_{pl} = 60$  ms. RF power ( $P_{RF} = 50 \div 200$  kW,  $F = 920$  MHz,  $\Delta t_{RF} = 6$  ms) is launched through two waveguide grill from the low field side of toroidal magnetic field. The maximum RF power  $P_{RF} = 200$  kW was more than two times higher than the ohmic heating power  $P_{OH} \sim 90$  kW. Figure 1 illustrates the LHCD effect for an RF pulse duration of 6 ms, initial plasma current of  $I_{pl} = 27$  kA, RF power of  $P_{RF} \sim 100$  kW, and plasma densities of  $\langle n_e \rangle = 10^{19}$  and  $2.0 \cdot 10^{19}$  m<sup>3</sup> (the solid and dashed curves, respectively).

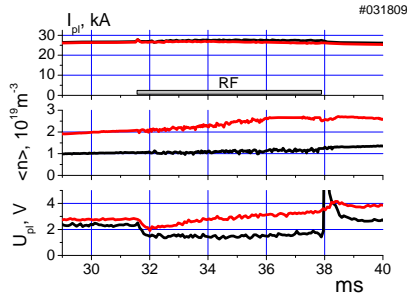


Figure 1. A typical waveform of LHCD experiment with  $I_{OH} = 27$  kA,  $P_{RF} = 100$  kW and different densities  $\langle n_e \rangle$ . Phase shift  $\Delta\phi = \pi/2$

The cross-section size of used waveguide for antenna is 21cm (height)  $\times$  2cm (width). The distance between waveguides is 2cm. The self consistent GRILL3D code taking into account finite waveguides height [3] is used for calculation of the spectra  $P(N_z)$  of the LHW excited in a plasma in front of the two waveguide grill. For given complex amplitudes of the waves propagating inside the waveguides

towards the plasma, the amplitudes of the reflected waves are computed self-consistently with account of the actual plasma response (plasma surface impedance found as a numerical solution of the plasma wave equation in a 1D inhomogeneous plasma). The real spectra of the excited waves are determined not just only by the supplied waveguides antenna geometry and by the phase shift  $\Delta\phi$  between incident waves in the left and right waveguides but also by edge plasma parameters, as well as depths and width of the sylphon bellows

corrugation of the liner wall. The spectra of LH waves is considered for three different phase

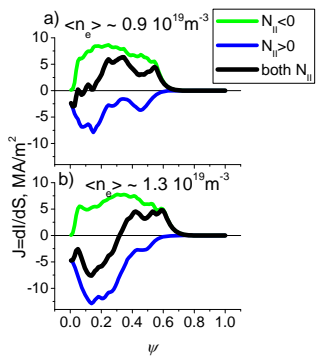


Fig. 2. Modeling by FRTC code the current density profile components.  $I_{PL} = 27\text{kA}$ ,  $P_{RF} = 100\text{kW}$ .  $\psi = \rho/a_L$

with allowance for the calculated spectrum  $P(N_z)$  of the excited LH waves and the measured plasma parameters, we found the value and direction of LHCD. The magnetic equilibrium of the plasma column was calculated using the ASTRA code for the radial plasma profiles and parameters of the FT-2 tokamak. The FRTC solves the wave equation for LH waves in the ray approximation in the cold plasma model, which is well applicable for frequencies exceeding the LH resonance frequency. The quasi-steady electric field and the action of LHCD on the equilibrium plasma parameters were not taken into account in these calculations. Nevertheless, the FRTC yielded a number of important results demonstrating

shifts between the antenna waveguides,  $\Delta\varphi = \pm \Delta\varphi/2$  and 0. For  $\Delta\varphi = \Delta\varphi/2$ , the RF pumping wave propagates oppositely to the plasma current (i.e., along the electron flow). Accordingly simulation the spectra of the slowed down RF waves are bidirectional (with respect to the plasma current) and that the RF spectrum  $P(N_z)$  has several maxima [1, 2]. For  $\Delta\varphi = \Delta\varphi/2$ , there are maxima at  $N_{||} = -9, -1.7, 3$ , and 20.

Using the Fast Ray Tracing Code (FRTC) [4]

specific features of LHCD. The calculated LHCD radial profiles  $J = dI/dS$ ,  $\text{MA/m}^2$ , where  $\psi$  is the relative radial coordinate of the magnetic surface is shown in Fig. 2. In the case of asymmetric excitation  $\Delta\varphi = \Delta\varphi/2$  for the initial plasma current  $I_{pl} = 27\text{kA}$ , central electron temperature  $T_e(0) = 450 \text{ eV}$ , and RF power  $P_{RF} = 100\text{kW}$ , the inductive plasma current at  $\langle n_e \rangle = 0.9 \cdot 10^{19} \text{ m}^{-3}$  can be completely replaced with the total LH-

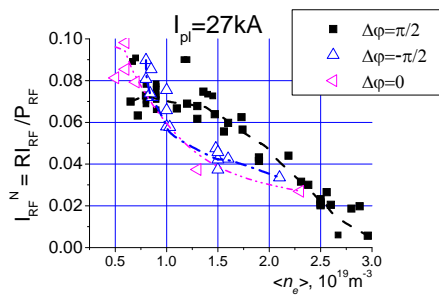


Fig. 3. Normalized LH driven current  $I_{RF}^N$  versus density at different  $\Delta\varphi$ . The injected LHW power is 100kW.

driven current, which is the sum of two oppositely directed currents. For higher plasma densities,  $1.5 \cdot 10^{19} \text{ m}^{-3}$   $n_e(0) = 2.6 \cdot 10^{19} \text{ m}^{-3}$ , the inductive current is replaced only partially,  $I_{RF} = 14.6\text{kA}$ . The simulations revealed the important role of the synergetic effect caused by the interaction of different spectral components of the excited RF waves. For the central electron temperature  $T_e(0) \sim 0.5 \text{ keV}$ , an LH wave with the slowing down factor  $N_{||} = -1.8$  efficiently drives the current only in the presence of even slower waves with  $N_{||} = -9$ . Waves

with  $N_{||} = -9$  alone are insufficient to drive the current; however, interacting with thermal electrons, they are capable of accelerating these electrons to velocities at which electrons efficiently interact with the main spectral component with  $N_{||} = -1.8$ . Thus, our simulations confirm that the FT-2 antenna system is capable of efficiently generating LH-driven currents, as was observed in experiment (Fig. 1).

In LH power scan experiments for CD efficiency, the plasma current was maintained at a constant value  $I_{pl}$  during LHCD. The experimental value of CD efficiency is calculated by the formula  $\eta_{exp} = \Delta U I_{pl} \langle n_e \rangle R / U_{OH} P_{LHW}$ , where the plasma current is  $I_{pl} = I_{rf} + I_{OH}$ ,  $I_{rf} = (-\Delta U / U_{OH}) I_P$  and the reduced loop voltage  $\Delta U = U_{LHW} - U_{OH}$ . The result of the LH power scan experiment for  $I_{pl} = 27\text{kA}$  shows that the LHCD efficiency really depends on the phase shift  $\Delta\varphi = \pm\pi/2, 0$  (see Fig. 2 in [1]). The higher efficiency  $\eta_{exp}$  is realized at  $\Delta\varphi = \pi/2$ . The

common tendency for  $\eta_{exp}$  is decreases with increasing LHW power. The dependence of the LHCD efficiency on the phasing  $\Delta\varphi$  is more pronounced when comparing the normalized currents  $I_{RF}^N = (-\Delta U / U_{OH}) I_{pl}$  for different plasma densities  $\langle n_e \rangle$  (Fig. 3). The current  $I_{RF}$  is seen to decrease with increasing density. In the density range  $\Delta n_e = (1.0 \div 2.0) 10^{19} \text{ m}^{-3}$ , the current  $I_{RF}^N$  for  $\Delta\varphi = \pi/2$  is substantially higher than that for other antenna phasings. The LHCD effect disappears at  $n_{LH} \approx 3 10^{19} \text{ m}^{-3}$  ( $n_{LH}$  ( $r=0\text{cm}$ )  $\approx 3.4 10^{19} \text{ m}^{-3}$ ) which approximately corresponds to the LH resonance density  $n_{LH}$  for  $f = 920 \text{ MHz}$ , at which the pumping

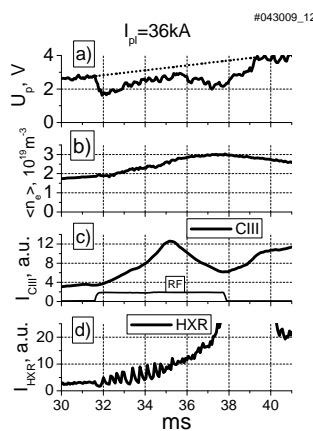


Fig.4 Changes of the  $U_{pl}$  (a), density  $\langle n_e \rangle$  (b), chord CIII intensity radiation (c) and HXR (2  $\div$  10 MeV) signal (d).  $P_{RF} = 100 \div 120 \text{ kW}$ ,  $T_e(0) = 500 \div 600 \text{ eV}$ . HXR signal demonstrates rise with the fan instability.

wave is linearly transformed into a warm plasma wave [6] and is then absorbed by ions.

It was shown, that at higher electron temperature (when the parametric effect is suppressed) CD efficiency decreasing and its termination will be determined by density rise and by impurity influx. Experiments are carried out at relatively large for installation plasma currents  $I_{pl} \sim 36 \text{ kA}$  ( $q \sim 4$ ), when initial central electron temperature  $T_e(0)$  reaches the value of  $\sim 0.5 \text{ keV}$ . Fig. 4 demonstrates the decrease in the loop voltage  $U_{pl}$ . LHCD is accompanied by an increase in the plasma density and the intensity of the spectral line of the CIII impurity. Moreover, the intensity of 2- to 10-MeV bremsstrahlung hard X-ray (HXR) emission [5] caused by the escape of runaway electrons onto the diaphragm and the chamber wall also undergoes typical variations. Additional impurity influx from the wall obviously resulted

from the fan or Parail-Pogutse instability (PPI) which produces the runaway electron flux at the limiter and the wall of the chamber [6]. When PPI spontaneous decreases the intensity of the CIII spectral line decreases abruptly during the RF pulse (at 35 ms). This is also accompanied by the additional reduction in the loop voltage (an increase in  $\Delta U = U_{OH} - U_{LHW}$ ). Thus, the LHCD efficiency increases substantially with decreasing impurity influx.

The loss of a fraction of runaway electrons during PPI can manifest itself as a change in the macroscopic plasma parameters, the diamagnetic and bolometric signals, and the loop voltage [6]. In our experiments, variations synchronous with HXR pulses were measured with

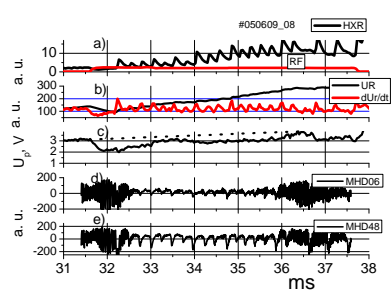


Fig. 5 Signal from the HXR detector (a), (b) signal  $U_R$  from the detector of the plasma column equilibrium along the major radius and its derivative  $dU_R/dt$ , (c) loop voltage  $U_R$ , and (d, e) signals from Mirnov coils during the RF pulse (shot no. #050609\_08).

the help of Mirnov coils and detectors of the plasma column equilibrium along the major radius and were also observed in the loop voltage signal. Figure 5 shows signals from two Mirnov coils located on the low-field side of the torus and separated by  $\theta = 20^\circ$  in the poloidal direction. Abrupt suppression of MHD oscillations takes place during LHCD. Moreover, spikes correlating with HXR pulses are observed in the probe signals. The marks of such spikes can also be observed in the control signal  $U_R$  and are most pronounced in its time derivative

$dU_R/dt$ . The analysis of the phase shift between signals from two spatially separated magnetic probes made it possible to determine the mode of MHD perturbation ( $m = 2, n = 1$ ). These perturbations develop on the resonance surface with  $q = 2$ , the radius of which, according to the calculations by the ASTRA code, is  $r \sim 5$  cm. Suppression of MHD oscillations indicates that LHCD leads to a change in the current density profile. According to model calculations (recall Fig. 2), the plasma current profile should change substantially (probably, it should broaden with increasing  $|grad|$  in the region  $r \sim 5 \div 6$  cm) in the course of LHCD. The problems related to variations in the current density profile and the observed change in the MHD stability of the plasma column is the subject of our further study.

This work was supported by the RFBR grants 08-02-00610, 08-02-00989, 10-02-00631, 07-02-92162-CNRS.

## References

- [1] S.I Lashkul, A.B. Altukhov, A.D. Gurchenko et al. 18th Topical Conf. on RF Power in Pl. (2009), Belgium
- [2] S.I Lashkul, A.B. Altukhov, A.D. Gurchenko et al. Plas. Phys. Reports, 2010, V. 36, No. 8 (to be published)
- [3] Irzak M.A., Shcherbinin O.N., Nuclear Fusion, 1995, v. 35, pp. 1341–1356.
- [4] A. D. Piliya and A. N. Saveliev, Preprint No. JET-R(98) 01 (JET Joint Undertaking, Abingdon, 1998).
- [5] V. N. Budnikov, V. V. Dyachenko et al., Proc. of the 25th EPS Conf., Prague, 1998, p 1360 (1998).
- [6] V. V. Parail and O. P. Pogutse, in @Reviews of Plasma Physics, Ed. by M. A. Leontovich and B. B. Kadomtsev (Atomizdat, Moscow, 1982; Consultants Bureau, New York, 1986), Vol. 11.